

NASA Grant Report
GTRI Report A5004/2000-4

Acoustic Absorption Characteristics of an Orifice With a Mean Bias Flow

K. K. Ahuja, R. J. Gaeta, Jr., and M. D'Agostino
*Georgia Institute of Technology, GTRI/ATASL
Acoustics and Aerospace Technologies Branch
Atlanta, Georgia 30332-0844*

Grant NAG1-1734

31 March 2000

Submitted to :

National Aeronautics and
Space Administration
Langley Research Center
Hampton, Virginia 23681-0001

Foreword/Acknowledgments

This report was prepared by the Acoustics and Aerospace Technologies Branch of the Aerospace, Transportation, and Advanced Systems Laboratory (ATASL) of Georgia Tech Research Institute (GTRI) for NASA Langley Research Center, Hampton, Virginia, under Grant NAG1-1734.

Mr. Mike Jones was the Project Manager for NASA Langley Research Center. GTRI's Project Director was Dr. K.K. Ahuja.

This work was carried out to obtain data for validation of bias flow codes being developed by High Technology Corporation. Special thanks are due to Dr. Meelan Choudhari of High Technology Corporation for suggesting this work. Note that this report is one of five separate volumes prepared to document the work conducted by GTRI under NASA Grant NAG1-1734. The GTRI report numbers, authors, and titles of each report are listed in the table below:

GTRI Report Number	Authors	Title
A5004/2000-1	Ahuja, K. K. and Gaeta, R. J.	Active Control of Liner Impedance by Varying Perforate Orifice Geometry
A5004/2000-2	Ahuja, K. K., Munro, S. E. and Gaeta, R. J.	Flow Duct Data for Validation of Acoustic Liner Codes for Impedance Eduction
A5004/2000-3	Ahuja, K. K., Gaeta, R. J. and D'Agostino, M. S.	High Amplitude Acoustic Behavior of a Slit-Orifice backed by a Cavity
A5004/2000-4	Ahuja, K. K., Gaeta, R. J. and D'Agostino, M. S.	Acoustic Absorption Characteristics of an Orifice With a Mean Bias Flow
A5004/2000-5	Ahuja, K. K., Cataldi, P. and Gaeta, R. J.	Sound Absorption of a 2DOF Resonant Liner with Negative Bias Flow

Table of Contents

<u>Description</u>	<u>Page</u>
Acknowledgments.....	i
Table of Contents.....	ii
List of Figures.....	iii
Executive Summary.....	iv
1.0 Introduction.....	1
2.0 Experimental Facilities and Approach.....	1
2.1 Normal Incidence Impedance Tube.....	1
2.2 Bias Flow Supply.....	2
2.3 Anechoic Termination.....	2
2.4 Hot Wire Measurements.....	2
3.0 Data Acquisition and Reduction.....	2
4.0 Mean Flow Characterization Upstream of Orifice.....	3
5.0 Results.....	3
5.1 Absorption Coefficient.....	3
5.2 Normal Incidence Impedance.....	4
6.0 Concluding Comments.....	5
7.0 References.....	6
Appendix A: Tabulated Orifice Velocities and Impedance Tube Velocity Profiles.....	18
Appendix B: Tabulated Orifice Acoustic Absorption Coefficient and Impedance.....	20

List of Figures

Figure	Page
Figure 1. Experimental set-up for impedance measurements of single orifice under bias flow conditions.....	7
Figure 2. Flow pattern for single orifice impedance tube measurements.....	8
Figure 3. Hot-Wire placement for upstream velocity profiles and orifice center velocity measurements.....	9
Figure 4. Measured orifice velocity versus bias volume flow rate with no acoustic excitation.....	10
Figure 5. Bias flow mean velocity profiles approximately 2 inches upstream of orifice in impedance tube.....	11
Figure 6. Effect of orifice bias flow Mach number on absorption coefficient.....	12
Figure 7. Nonlinearity of orifice: Acoustic impedance as a function of orifice velocity with NO bias flow present.....	13
Figure 8. Effect of incident sound amplitude on absorption coefficient with bias flow.....	14
Figure 9. Effect of Strouhal number on absorption coefficient.....	15
Figure 10. Effect of bias flow Mach number on normalized resistance.....	16
Figure 11. Effect of bias flow Mach number on	17

Executive Summary

The objective of the study reported here was to acquire acoustic and flow data for numerical validation of impedance models that simulate bias flow through perforates. The impedance model is being developed by researchers at High Technology Corporation. This report documents normal incidence impedance measurements a singular circular orifice with mean flow passing through it. All measurements are made within a 1.12 inch (28.5 mm) diameter impedance tube. The mean flow is introduced upstream of the orifice (with the flow and incident sound wave travelling in the same direction) with an anechoic termination downstream of the orifice. Velocity profiles are obtained upstream of the orifice to characterize the inflow boundary conditions. Velocity in the center of the orifice is also obtained. All velocity measurements are made with a hot wire anemometer and subsequently checked with mass flow measurements made concurrently. All impedance measurements are made using the Two-Microphone Method. Although we have left the analysis of the data to the developers of the impedance models that simulate bias flow through perforate, our initial examination indicates that our results follow the trends consistent with published theory on impedance of perforates with a steady bias flow.

1.0 Introduction

Personnel at High-Technology Corporation in Hampton, VA, are developing computational aeroacoustic codes to simulate the effects of flow on the impedance of orifices. Flow through acoustic liners that incorporate perforates have the potential for high acoustic attenuation as well as control of the frequency of attenuation^{1,2}. Acoustic data and corresponding flow data to validate these codes do not exist and it is the objective of this report to provide such data. In order to facilitate the numerical validation, GTRI's high intensity impedance tube was modified to provide an anechoic termination downstream of the orifice and provide measurements of velocity profiles upstream of the orifice. In addition, velocities in the center of the orifice were also obtained. The steady flow was supplied by a suction device downstream of the orifice which created a negative bias flow (mean flow travelling in same direction as incident acoustic wave).

2.0 Experimental Approach and Facilities

The behavior of a single circular orifice under the influence of bias flow was studied using a normal incidence impedance tube that had several unique features: 1) The tube allowed for a source of air to enter upstream of the orifice [travelling in the same direction as the incident acoustic wave] as well as an exhaust port downstream of the orifice; 2) it was provided with an anechoic termination downstream of the orifice; and 3) it had a port that allowed a hot-wire to be placed in the center of the orifice. The mean mass flow rate in the impedance tube was measured with a venturi meter. A hot-wire anemometer was used to measure mean flow profiles upstream of the orifice in the impedance tube. The anechoic termination assured that the measured impedance was due to the orifice (and surrounding plate) alone.

The orifice under consideration was circular (diameter = 0.1954 in.) and was placed in a 2.5-inch diameter aluminum plate that was approximately 0.032-inches thick. The orifice plate was placed between flanges on the impedance tube at the measurement reference plane. The controlled variables in this experiment were acoustic frequency, amplitude, and bias flow velocity. Table I shows the test conditions covered in the present study. For each case, the reflection coefficient, absorption coefficient and acoustic impedance were measured.

Frequency [Hz]	Incident Amplitude [dB]	Orifice Mach Number
1000	110, 120, 130, 145	0.00, 0.05, 0.10, 0.15, 0.20
2000	110, 120, 130, 145	0.00, 0.05, 0.10, 0.15, 0.20
3000	110, 120, 130, 145	0.00, 0.05, 0.10, 0.15, 0.20
4000	110, 120, 130, 145	0.00, 0.05, 0.10, 0.15, 0.20
5000	110, 120	0.00, 0.05, 0.10, 0.15, 0.20
6000	110, 120, 130, 145	0.00, 0.05, 0.10, 0.15, 0.20

Table I. Test conditions for single orifice with bias flow.

2.1 Normal Incidence Impedance Tube

The normal incidence acoustic impedance measurements were made using the Two Microphone Method as originally described by Chung and Blaser³. Our impedance tube was a steel tube whose general specifications are detailed in reference 4. The tube's inner diameter is 1.12 inches. Figure 1 shows the basic impedance tube set-up for the present experiments.

2.2 Bias Flow Supply

Bias flow was supplied to the impedance tube via a suction device. An air amplifier, similar to the one described in the 2DOF tests of reference 2, was used to create negative pressure in a conduit. The conduit was attached to the impedance tube with two 0.375 inch pressure ports on the tube downstream of the orifice (see figure 1). Air was drawn in from the inlet ports near the acoustic driver, pushed through the orifice and out the tube to the air amplifier. A Flow-Dyne venturi flow meter was placed in-line to measure the mass flow rate in the impedance tube. Figure 2 shows the impedance tube and the path of the bias flow.

2.3 Anechoic Termination

Elimination of acoustic reflection downstream of the orifice was accomplished by placing sound absorbing material at the impedance tube's termination. An 11-inch long wedge of Pyrell foam was followed by a large box filled with fiberglass (see Figure 1). Tests were conducted to verify the extent of the reflection back to the reference plane where the orifice was installed. Using a broadband noise as input, an absorption coefficient of 0.96 was achieved at 1000 Hz. Absorption coefficients of 0.99 were achieved above 1000 Hz with the anechoic termination in place.

2.4 Hot-Wire Measurements

Two sets of hot-wire measurements were made. A traverse of the flow-field perpendicular to the axis of the impedance tube upstream of the orifice characterized the approaching mean flow profile. The hot-wire probe was placed in one of the microphone ports and traversed across the tube. Measurements of the velocity in the center of the orifice were also made. A special port was installed downstream of the orifice that allowed the hot-wire probe to enter the tube to be placed in the orifice's center. Figure 3 shows how the hot-wire probe was arranged in the impedance tube for velocity measurements.

3.0 Data Acquisition and Reduction

Acoustic impedance was determined using acoustic measurements from two microphones that were flush mounted near the reference plane where the orifice was placed (see Figure 1). The cross spectral data from these signals were processed with an HP 3667A Signal Analyzer and then used in the Chung and Blaser algorithm for the Two Microphone Method processed on a Pentium II platform. A sinusoidal input from a function generator was supplied to the JBL acoustic driver via a Carvin Amplifier. Acoustic impedance was obtained with and without bias flow present. All acoustic data was obtained with no hot-wire present in the impedance tube. The amplitude of the discrete tone was fixed at constant incident sound pressure levels prescribed in Table I. The incident amplitude was determined from the measured impedance via the method outlined in Chung and Blaser. It took several iterations before finding the correct driver voltage that produced the correct incident sound pressure level, but once found, the voltage was matched for all bias flow conditions.

The bias flow was controlled by adjusting the air amplifier supply pressure. In order to set the bias flow magnitude to the values prescribed in Table I, a series of hot-wire measurements were made with no acoustic excitation. The volume flow rate was determined from pressure measurements made on the venturi using standard compressible flow theory. Real time data was acquired with a LabView program that converted the pressure

measurements into a volume flow rate. With the hot-wire placed in the center of the orifice, the bias flow rate was adjusted until a relationship between flow rate and orifice velocity could be determined. Thus, a given orifice Mach number corresponded to a specific mass flow rate that could be set with the air amplifier. The Mach number was referenced to the ambient temperature *outside* of the impedance tube. Figure 4 shows the relationship between volume flow rate and orifice velocity. For comparison, the calculated orifice velocity from continuity is shown as well. There is good agreement between the hot-wire and the calculated values, with differences attributed to the unknown orifice discharge coefficient and mass flow measurement accuracy.

4.0 Mean Flow Characterization Upstream of Orifice

Before acoustic impedance measurements were made, the flow approaching the orifice was traversed to quantify the mean velocity profile. The hot-wire was traversed until it almost touched the opposite wall from its entrance point. However, in order to maintain a proper seal, the hot-wire could not be placed near the entrance wall. In spite of this, almost 85% of the tube diameter was traversed with the probe. For the bias flow orifice Mach numbers indicated in Table I, mean flow profiles were obtained for boundary condition information for future numerical studies. Figure 5 shows these velocity profiles approximately 2 inches upstream of the orifice.

5.0 Results

5.1 Absorption Coefficient

The absorption coefficient was calculated from the measured reflection coefficient using the relationship:

$$\alpha = 1 - |R|^2$$

and plotted as a function of orifice bias flow Mach number. The results are shown in Figure 6, noting that a smooth curve was fit through the data points. Also note that data for 130 dB and 145 dB at 5000 Hz could not be obtained due to irregularity in the acoustic driver. Figures 6a-6d show data for 110 dB, 120 dB, 130 dB, and 145 dB, respectively.

One feature of the data is that, for the frequencies tested, there appears to be a relative minima and maxima for a given frequency as the bias flow is increased. At 1000 Hz, the maximum absorption occurs at $M = 0.05$ (~ 17 m/s) and at 2000 Hz it occurs at $M = 0.1$ (~ 34 m/s) with the caveat that at 145 dB at these two frequencies, increasing bias flow diminishes the absorption. As frequency is increased, the bias flow Mach number at which maximum absorption occurs increases.

Another feature of the absorption data is that it appears to be relatively independent of amplitude of the incident wave. This can be more clearly seen by examining the nonlinearity of the orifice with no bias flow present. Figure 7 shows the normalized resistance and reactance of the orifice as a function of the rms velocity in the center of the orifice. These velocities correspond to incident sound pressure levels listed in Table I. (Data for 5000 Hz is not shown because the 130 dB & 145 dB cases were not obtained.) The impedance is relatively independent of the amplitudes tested when the orifice velocities were below 10 m/s. Only 1000 Hz and 2000 Hz exhibit nonlinearity when the incident amplitude was 145 dB. This is consistent with the

absorption data shown in Figure 6, and is even more evident in Figures 8a through 8c that show the absorption coefficient as a function of incident level for each frequency, respectively.

The absorption of sound by the orifice with a bias flow jet has been treated analytically by Howe⁵ in the form of a bias flow through a rigid perforated screen with no backing cavity. Howe showed that for a given level of bias flow, the absorption coefficient maximizes as the Strouhal number [$S_t = \omega d_o / U_o$] tends towards zero. He found that for normal incidence, the maximum absorption occurs when

$$\frac{\sigma}{M_o} = 1$$

where σ is the perforate porosity and M_o is the bias flow Mach number. Furthermore, when this ratio is unity, the maximum absorption coefficient that can be achieved is shown to be 0.5 for a perforated screen with bias flow. For values σ / M_o greater than or less than unity, the maximum absorption is less than the value at $\sigma / M_o = 1$. At a given σ / M_o , the absorption coefficient decreases rapidly as the Strouhal approaches unity. Howe explains this behavior as follows: When the vorticity length scale [$\sim U_o / \omega$] is small, velocities induced by successive vortex rings mostly cancel, except in the vicinity of the orifices. At low Strouhal numbers, the vorticity of one sign can stretch many orifice diameters downstream and produces a strong effect on the flow. Thus, Howe concludes that vorticity production at very high frequencies has a negligible influence on the fluctuating flow.

In the present experiments, a single orifice rather than a perforate is used and the highest ratio of porosity to bias flow Mach number is 0.6 [$\sigma = 0.03$, $M_o = 0.05$]. However, the trends that Howe predict are evident in the present data as shown in Figures 9a through 9d, which show the absorption coefficient as a function a Strouhal number and σ / M_o . Note, as σ / M_o tends toward unity, the absorption levels increase. Also, the rapid decrease in absorption coefficient as the Strouhal number approaches one is evident. It should be noted that not enough data were obtained at the low Strouhal number region at the lowest bias flow Mach number tested and at the high bias flow Mach number not enough data were obtained in the higher Strouhal number region to "flesh out" the trend. However, the trend exhibited by the $\sigma / M_o = 0.3$ curves in Figures 9a through 9d, are indicative of Howe's prediction. It is also evident that absorption coefficients above 0.5 were measured, which are greater than predicted.

We hope that these data will serve a useful purpose in validating other's theoretical models.

5.2 Normal Incidence Impedance

Together, figures 10 and 11 show the normalized impedance of the single orifice under the influence of a steady bias flow by displaying normalized resistance and reactance, respectively, as a function of bias flow Mach number. These data were used to compute the reflection coefficient and thus the absorption coefficient data. Note that the resistance, in general, increases with increasing bias flow Mach number. As the frequency increases, the bias flow Mach number at which the minimum reactance occurs increases. This is consistent with the trend in the absorption coefficient data (see Figure 6). Recall that the as the frequency increased, the value of bias flow Mach number at which maximum absorption occurred increased. The absorption coefficient is large when the normalized impedance of the orifice plate is closest to matching the impedance of air (ρc)

6.0 Concluding Comments

Note that the purpose of acquiring the data presented here was to provide it to High Technology Corporation researchers for validating numerical models being developed by them. The data has been provided to them and NASA Langley Technical monitor for use by others.

7.0 References

1. Dean, P. D. & Tester, B. J. Duct Wall Impedance Control as an Advanced Concept for Acoustic Suppression, NASA Contractor Rept. CR-134998, Nov. 1975
2. Cataldi, P., Ahuja, K. K. , and Gaeta, R. J. , Enhanced Sound Absorption through Negative Bias Flow, AIAA Paper No. 99-1879, Presented at the 5th AIAA/CEAS Aeroacoustics Conference, May 10-12, 1998, Seattle, WA.
3. Chung, J. Y. and Blaser, D. A. Transfer Function Method of Measuring In-Duct Acoustic Properties: I. Theory Journal of the Acoustic Society of America, Volume 68, No. 3, Sept., 1980.
4. Gaeta, R. J. Liner Impedance Modification by Varying Perforate Orifice Geometry Ph.D. Thesis, Georgia Institute of Technology, 1998.
5. Howe, M. S. Acoustics of Fluid-Structure Interactions Cambridge University Press, Cambridge, UK, 1998.

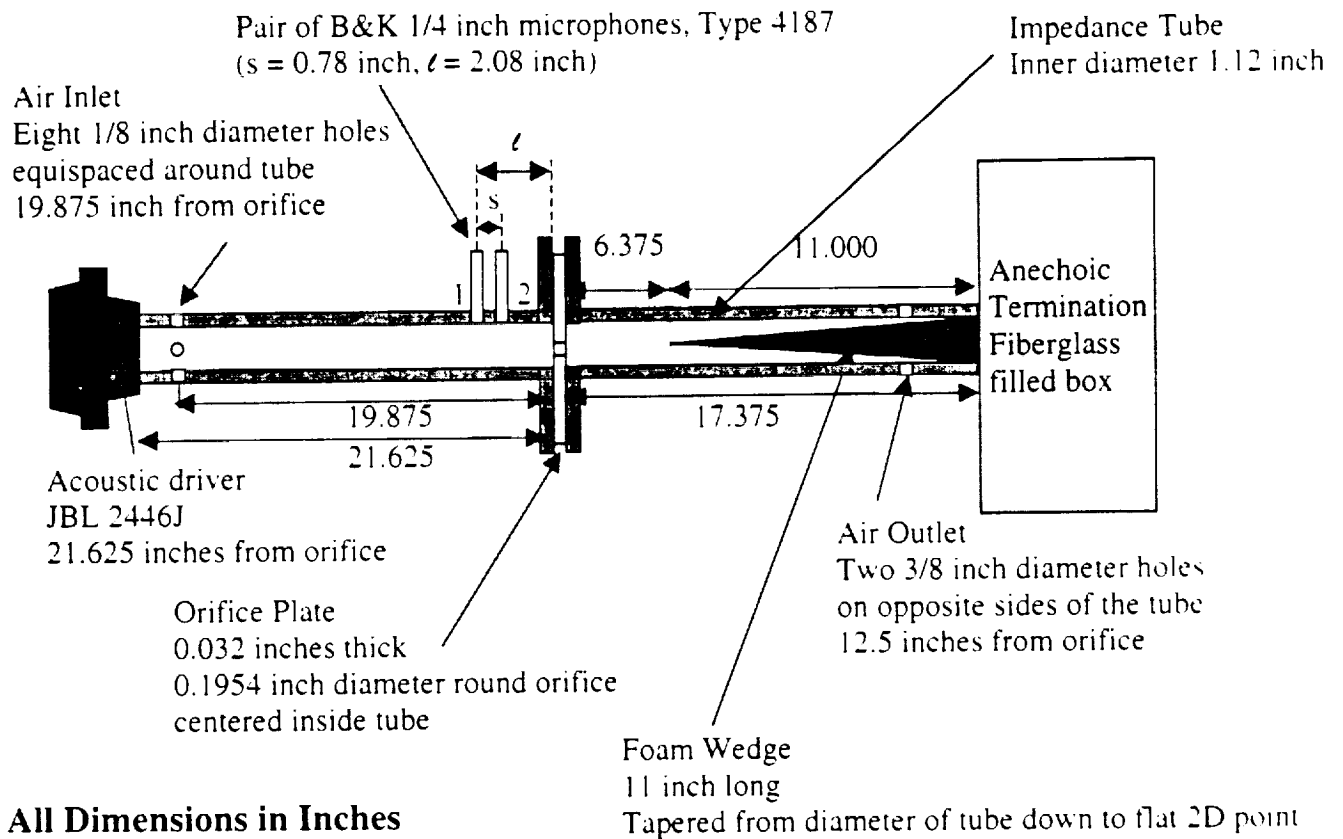


Figure 1. Experimental set-up for impedance measurements of single orifice under bias flow conditions

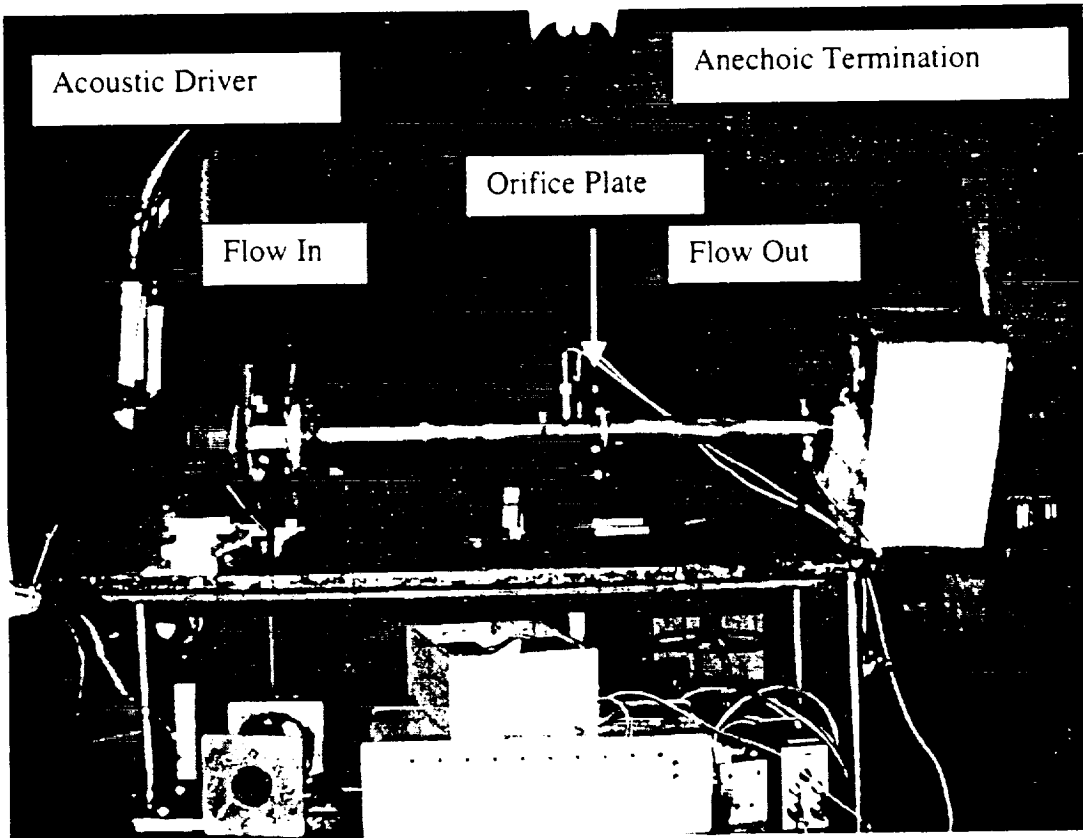
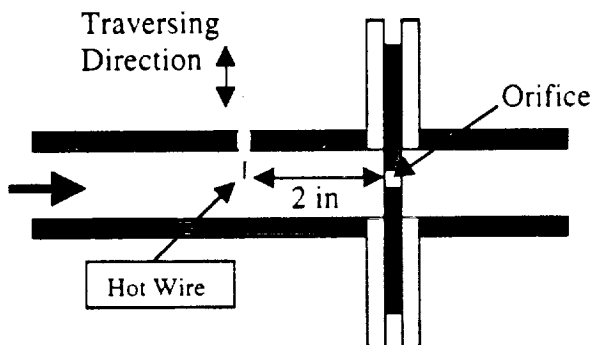
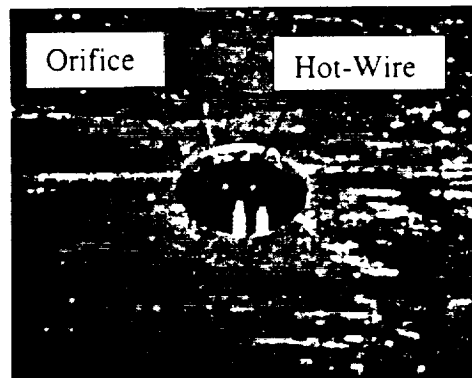
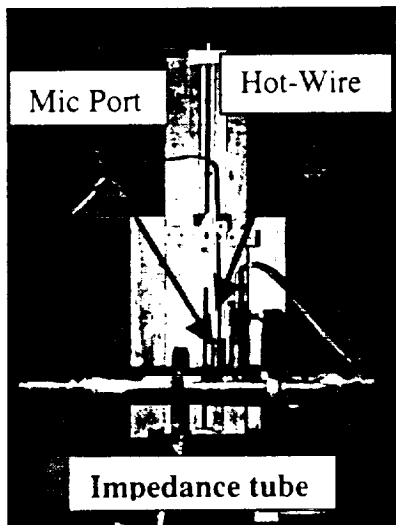
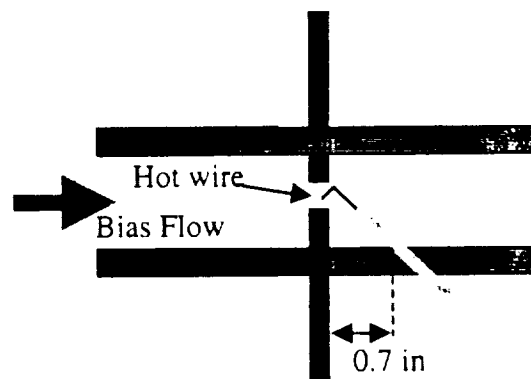


Figure 2. Flow pattern for single orifice impedance tube measurements.



Hotwire Placement for Velocity Profile



Hot-wire Placement In Orifice Center

Figure 3. Hot-Wire placement for upstream velocity profiles and orifice center velocity measurements.

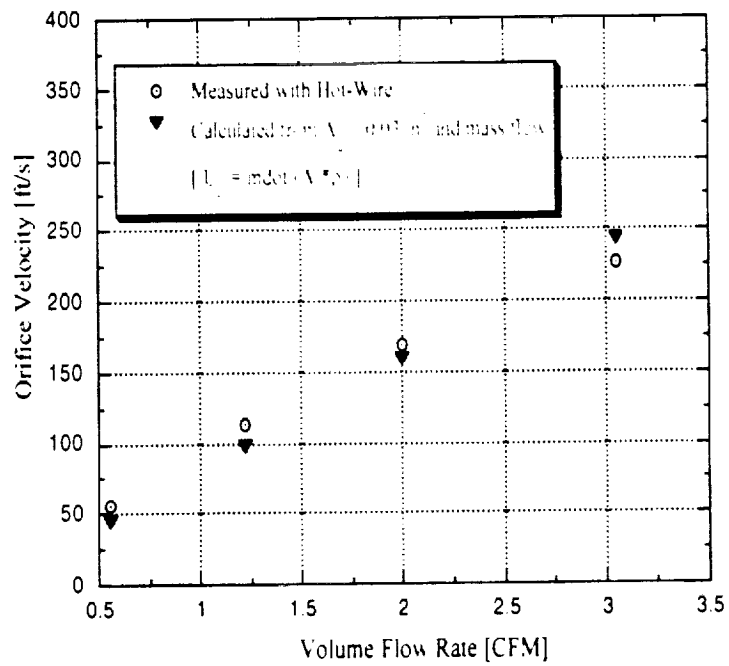


Figure 4. Measured orifice velocity versus bias volume flow rate with no acoustic excitation.

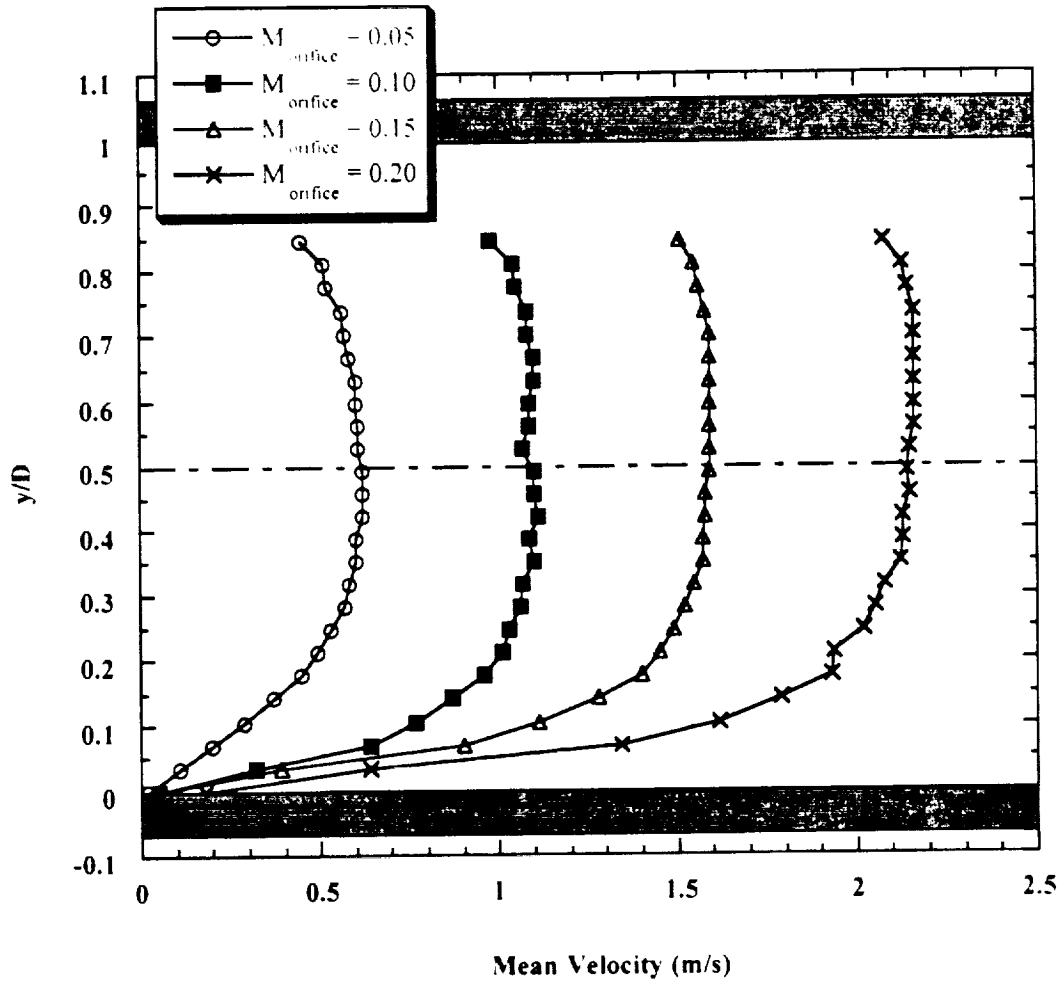


Figure 5. Bias flow mean velocity profiles approximately 2 inches upstream of orifice in impedance tube.

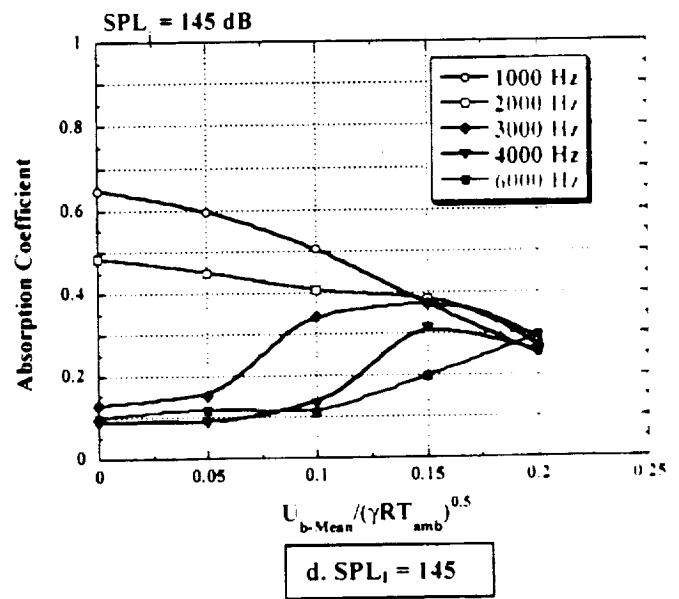
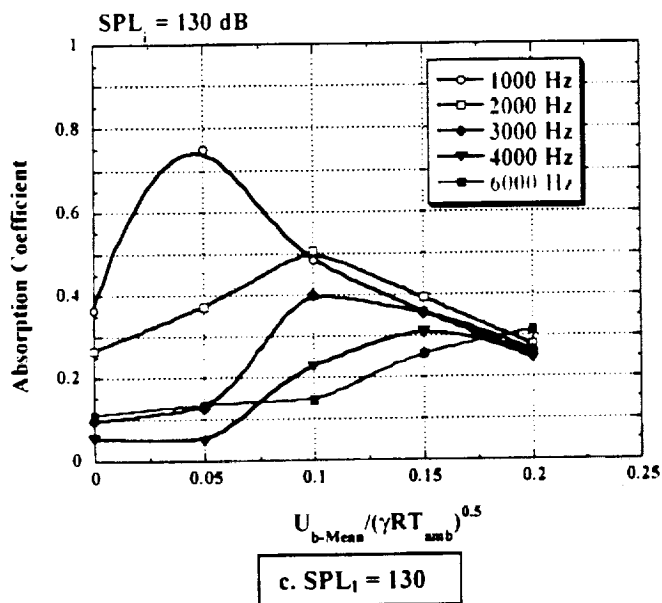
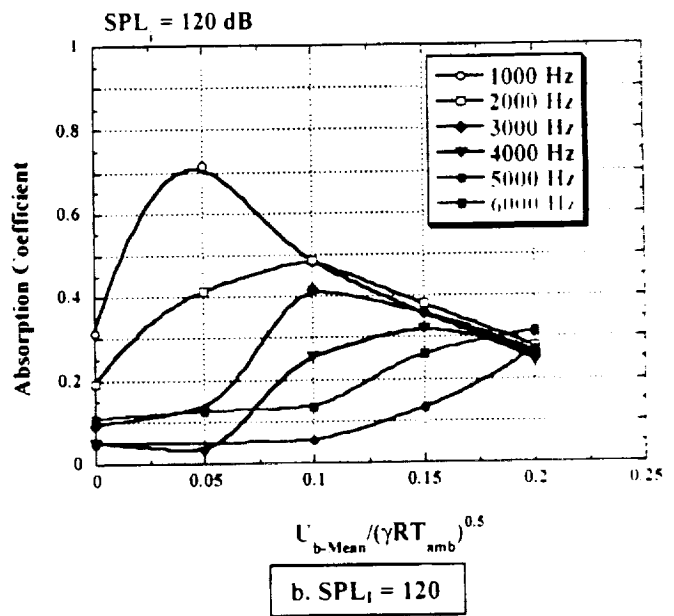
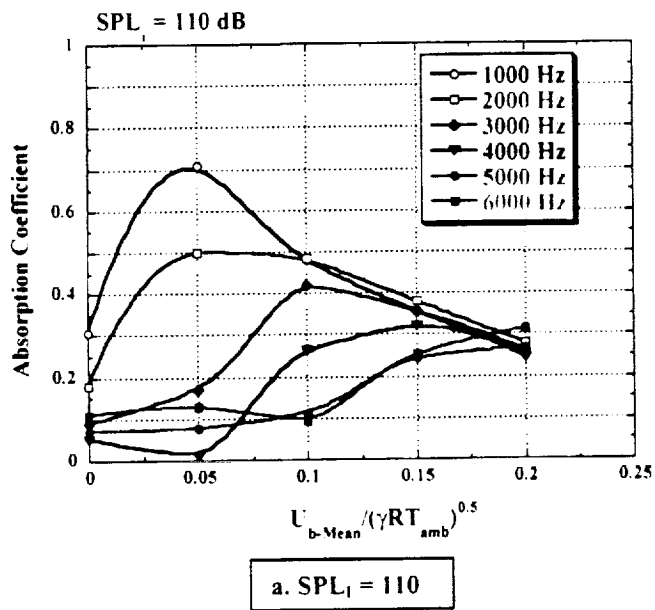


Figure 6. Effect of orifice bias flow Mach number on absorption coefficient.

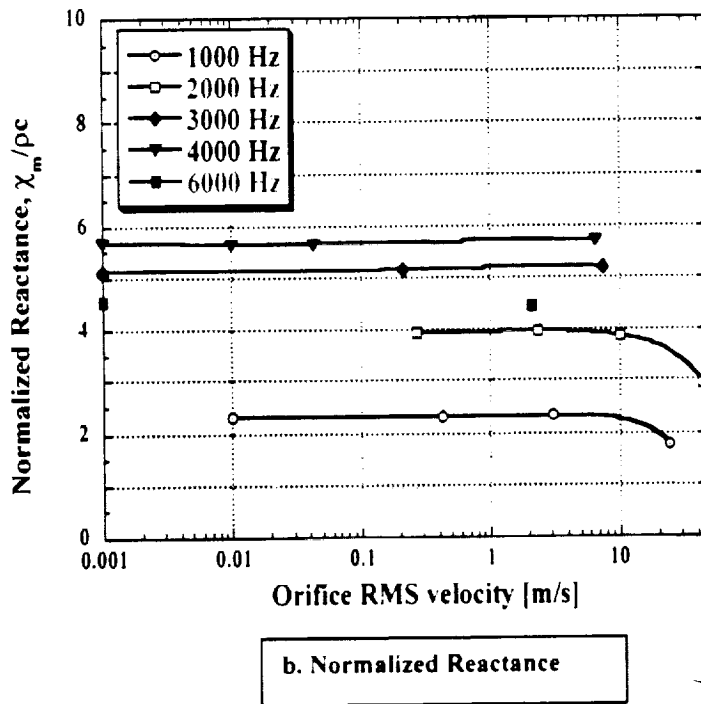
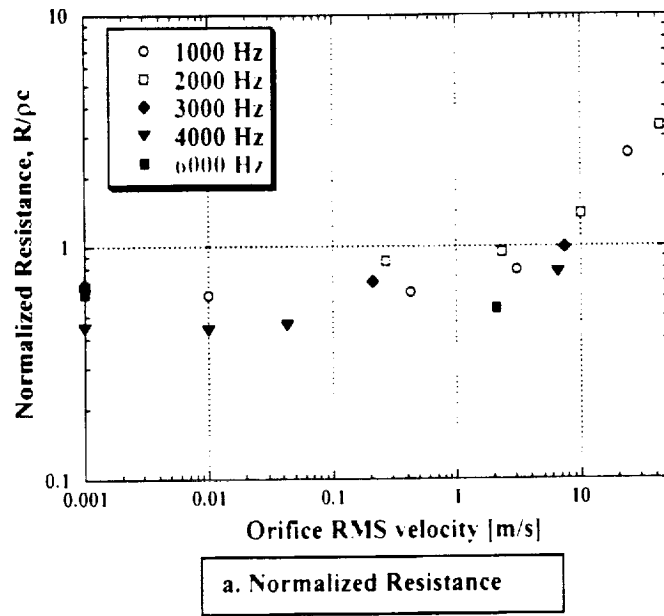


Figure 7. Nonlinearity of orifice: Acoustic impedance as a function of orifice velocity with NO bias flow present

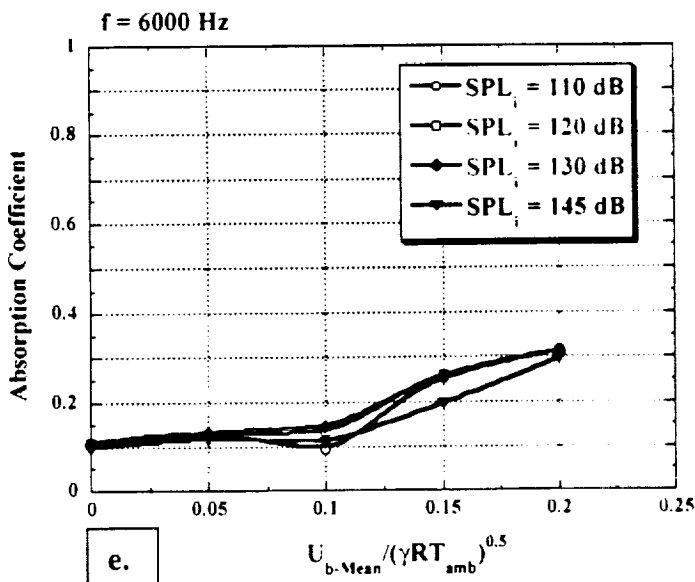
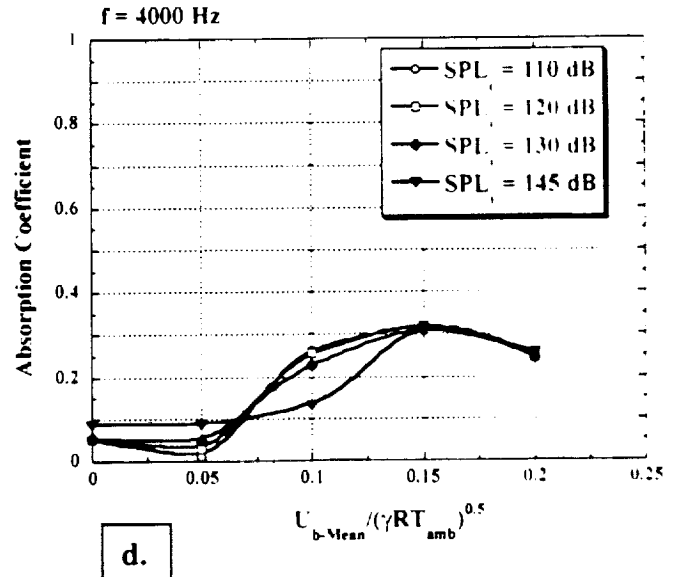
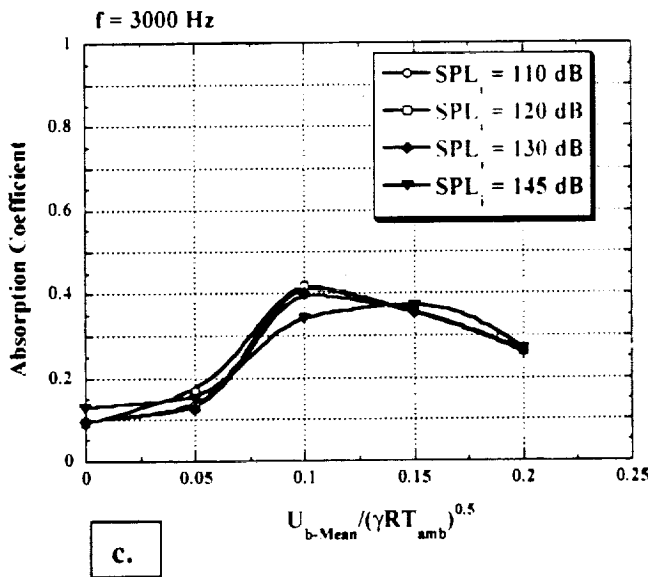
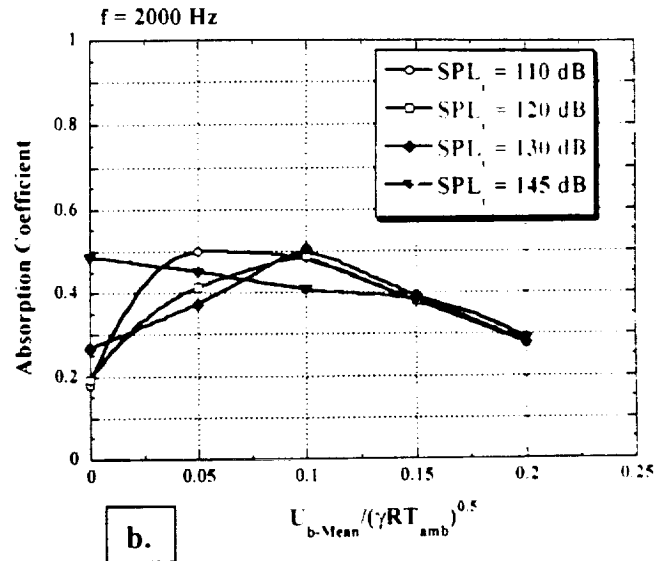
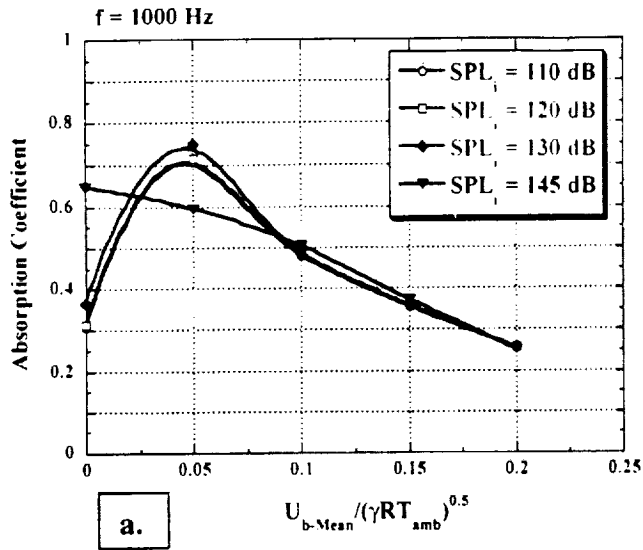
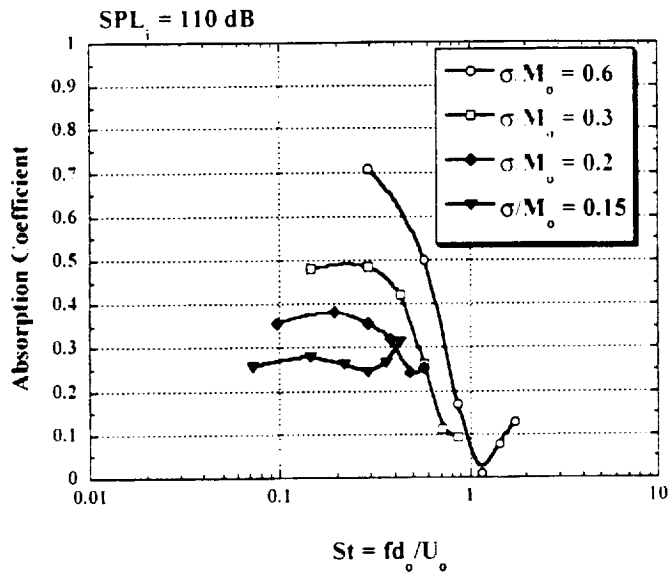
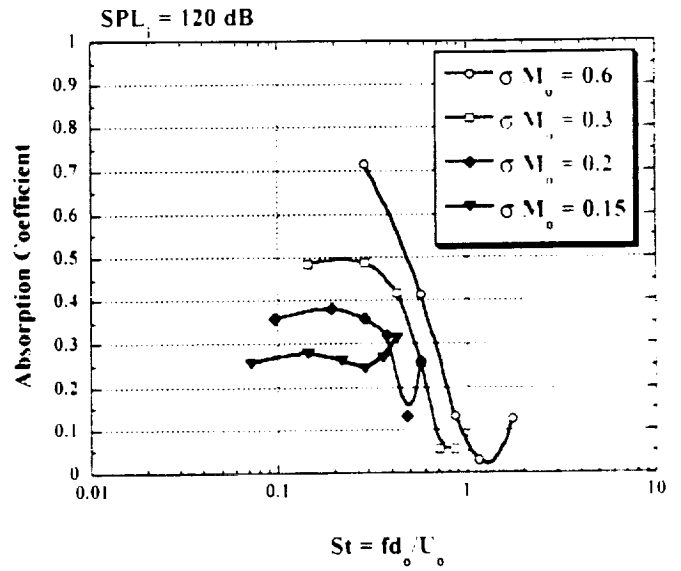


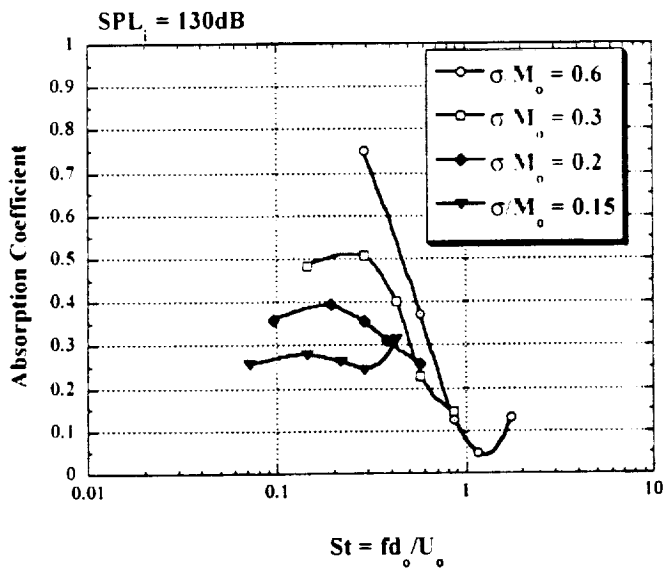
Figure 8. Effect of incident sound amplitude on absorption coefficient with bias-flow.



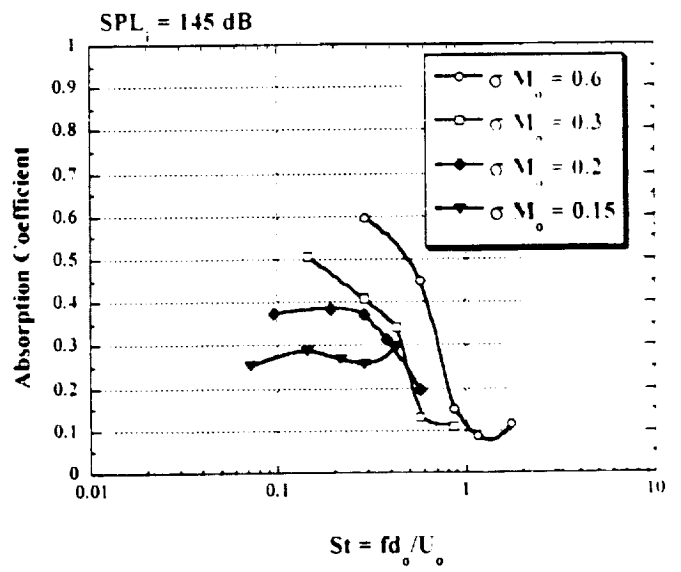
a. SPL_i = 110 dB



b. SPL_i = 120 dB

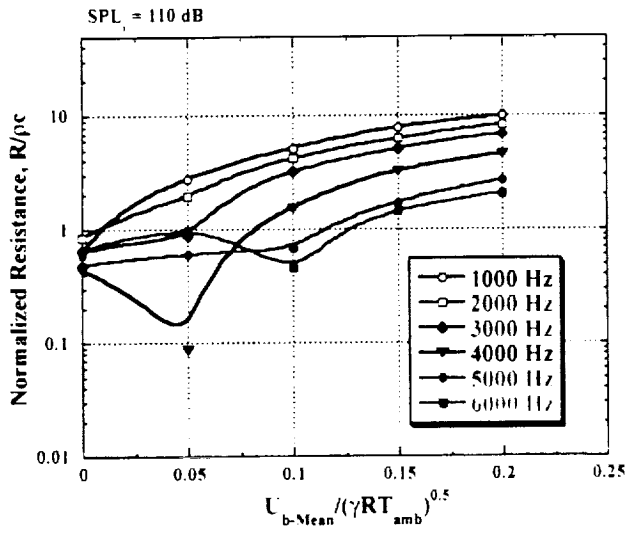


c. SPL_i = 130 dB

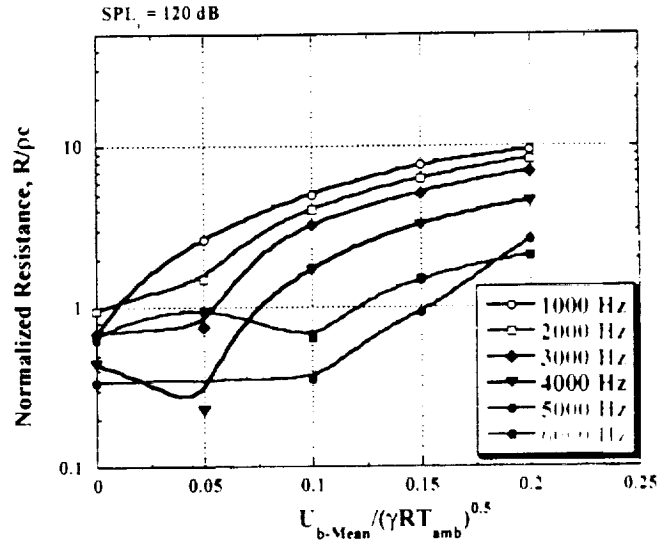


d. SPL_i = 145 dB

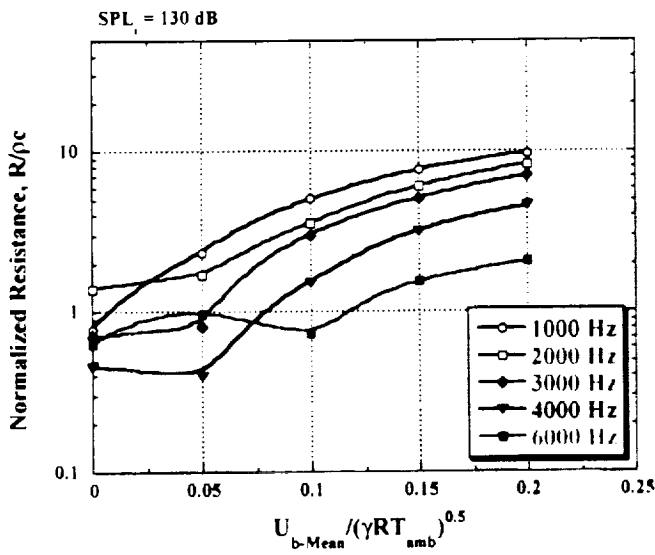
Figure 9. Effect of Strouhal number on absorption coefficient



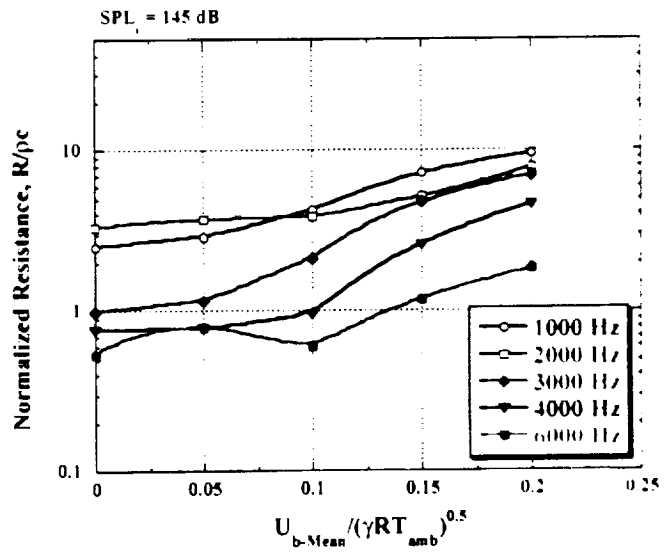
a. $SPL_1 = 110$ dB



b. $SPL_1 = 120$ dB

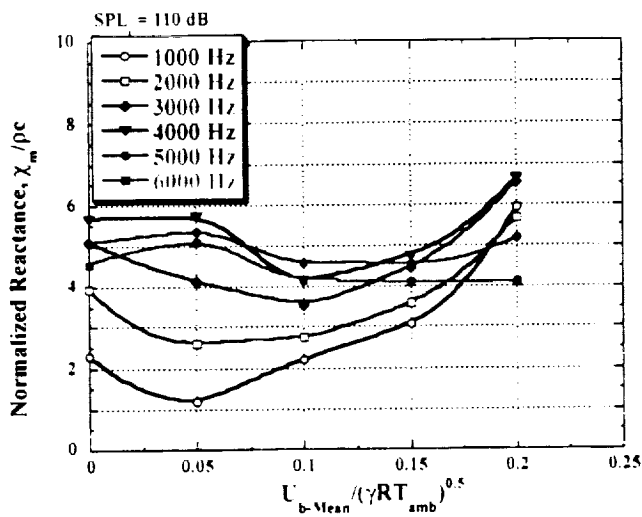


c. $SPL_1 = 130$ dB

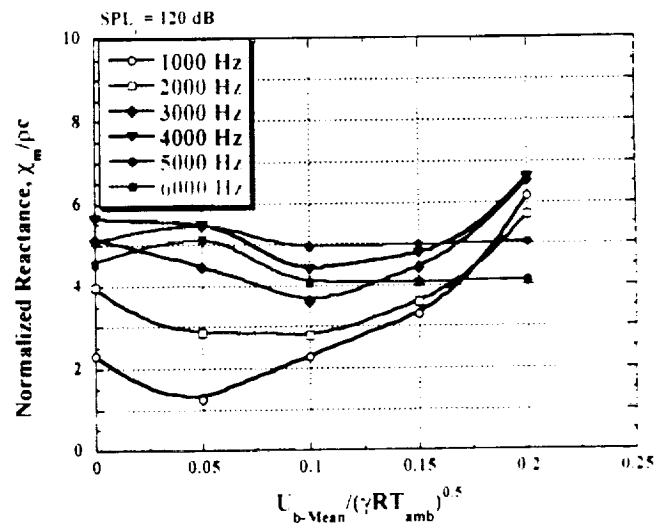


d. $SPL_1 = 145$ dB

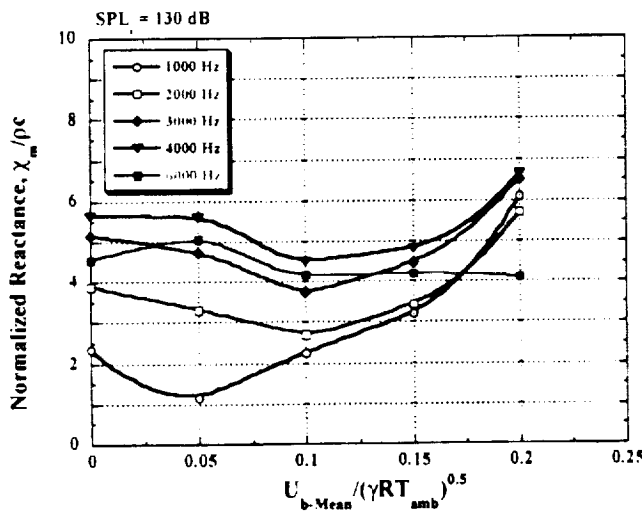
Figure 10. Effect of bias flow Mach number on normalized resistance.



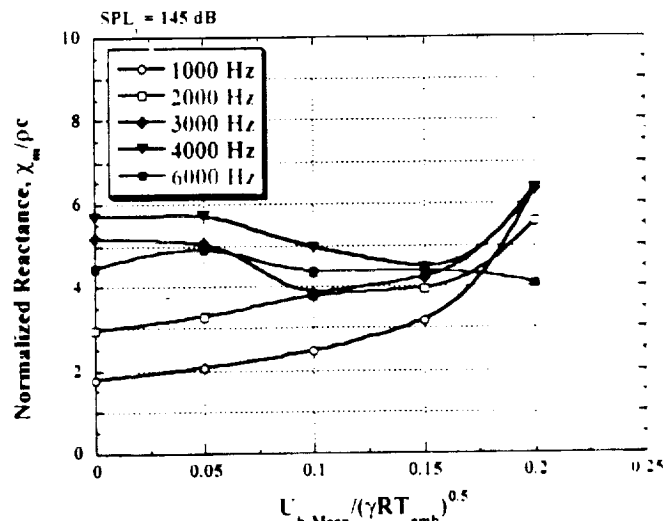
a. $SPL_1 = 110$ dB



b. $SPL_1 = 120$ dB



c. $SPL_1 = 130$ dB



d. $SPL_1 = 145$ dB

Figure 11. Effect of bias flow Mach number on normalized reactance.

Appendix A

Tabulated Orifice Velocities and Impedance Tube Velocity Profiles

Measured Orifice Mean Velocities and Volume Flow Rates

Mo	Vol. Flow [CFM]	Uo [ft/s]
0.050000	0.56000	56.50
0.10000	1.2200	113.00
0.15000	2.0000	169.50
0.20000	3.0500	226.00

Mean Velocity Profiles Measured 2.08 inches Upstream of Orifice

y/D	Mo = 0.05	Mo = 0.10	Mo = 0.15	Mo = 0.20
0.0000	0.020000	0.050000	0.050000	0.10000
0.03000	0.11000	0.32000	0.39000	0.64000
0.07000	0.20000	0.64000	0.90000	1.3400
0.10500	0.29000	0.77000	1.1100	1.6200
0.14100	0.37000	0.87000	1.2800	1.7900
0.17600	0.45000	0.96000	1.4000	1.9300
0.21100	0.49000	1.0100	1.4500	1.9400
0.24600	0.53000	1.0300	1.4900	2.0200
0.28100	0.57000	1.0600	1.5200	2.0500
0.31600	0.58000	1.0700	1.5500	2.0500
0.35200	0.60000	1.1000	1.5700	2.1200
0.38700	0.60000	1.0900	1.5700	2.1300
0.42200	0.62000	1.1100	1.5800	2.1300
0.45700	0.62000	1.1000	1.5800	2.1500
0.49200	0.62000	1.1000	1.5900	2.1400
0.52700	0.61000	1.0700	1.5900	2.1500
0.56200	0.61000	1.0900	1.5900	2.1600
0.59800	0.60000	1.0900	1.5900	2.1600
0.63300	0.60000	1.1000	1.5900	2.1600
0.66800	0.58000	1.1000	1.5900	2.1600
0.70300	0.57000	1.0800	1.5900	2.1600
0.73800	0.56000	1.0800	1.5800	2.1600
0.77400	0.52000	1.0500	1.5600	2.1400
0.80900	0.51000	1.0400	1.5500	2.1300
0.84400	0.45000	0.98000	1.5100	2.0800

Appendix B

Tabulated Orifice Acoustic Absorption Coefficient and Impedance

Frequency = 1000 Hz

SPLi = 110 dB

Mo	Absorption Coefficient	R/pc	χ pc
0.0000	0.30690	0.61130	2.3173
0.050000	0.70960	2.7742	1.1507
0.10000	0.47960	5.2109	0.5112
0.15000	0.35670	7.8988	3.0649
0.20000	0.25660	9.9403	5.9379

SPLi = 120 dB

Mo	Absorption Coefficient	R/pc	χ pc
0.0000	0.31470	0.63250	2.3185
0.050000	0.71420	2.5965	1.2674
0.10000	0.48450	5.0068	0.5214
0.15000	0.35820	7.6050	3.2987
0.20000	0.25700	9.4707	6.1470

SPLi = 130 dB

Mo	Absorption Coefficient	R/pc	χ pc
0.0000	0.36520	0.78610	2.3283
0.050000	0.74890	2.3438	1.1563
0.10000	0.48470	5.0434	2.2587
0.15000	0.35920	7.6592	3.2121
0.20000	0.25550	9.7489	6.0987

SPLi = 145 dB

Mo	Absorption Coefficient	R/pc	χ pc
0.0000	0.64760	2.5199	1.7819
0.050000	0.59600	2.9108	2.0598
0.10000	0.50570	4.2526	2.4590
0.15000	0.37380	7.1671	3.1609
0.20000	0.25200	9.5545	6.3433

Frequency = 2000 Hz

SPLi = 110 dB

Mo	Absorption Coefficient	R/pc	χ pc
0.0000	0.18020	0.85770	3.9480
0.050000	0.50170	1.9478	2.6151
0.10000	0.48420	4.2263	2.7569
0.15000	0.38090	6.3074	3.5801
0.20000	0.27900	8.3434	5.6869

SPLi = 120 dB

Mo	Absorption Coefficient	R/pc	χ pc
0.0000	0.19270	0.94150	3.9710
0.050000	0.41380	1.4906	2.8048
0.10000	0.48690	4.0486	2.7878
0.15000	0.38100	6.2969	3.5873
0.20000	0.27890	8.3258	5.6938

SPLi = 130 dB

Mo	Absorption Coefficient	R/pc	χ pc
0.0000	0.26680	1.3623	3.8789
0.050000	0.37340	1.7183	3.3193
0.10000	0.50810	3.5790	2.6845
0.15000	0.39300	6.0735	3.4337
0.20000	0.27920	8.2706	5.7054

SPLi = 145 dB

Mo	Absorption Coefficient	R/pc	χ pc
0.0000	0.48520	3.3292	3.9502
0.050000	0.45010	3.7061	3.2844
0.10000	0.40640	3.8957	3.7917
0.15000	0.38550	5.1697	3.8472
0.20000	0.28790	7.7858	5.5677

Frequency = 3000 Hz

SPLi = 110 dB

Mo	Absorption Coefficient	R/pc	χ /pc
0.0000	0.089900	0.64850	5.1114
0.050000	0.17010	0.88270	4.1486
0.10000	0.42160	3.2371	3.5722
0.15000	0.35680	5.1122	4.4672
0.20000	0.26180	6.9628	6.5569

SPLi = 120 dB

Mo	Absorption Coefficient	R/pc	χ /pc
0.0000	0.093300	0.68280	5.1424
0.050000	0.13110	0.75630	4.4710
0.10000	0.41720	3.2297	3.6185
0.15000	0.35840	5.1358	4.4356
0.20000	0.26260	7.0191	6.5262

SPLi = 130 dB

Mo	Absorption Coefficient	R/pc	χ /pc
0.0000	0.095200	0.70110	5.1542
0.050000	0.12490	0.80390	4.7418
0.10000	0.40090	3.0313	3.7404
0.15000	0.35560	5.1272	4.4869
0.20000	0.26300	7.0392	6.5143

SPLi = 145 dB

Mo	Absorption Coefficient	R/pc	χ /pc
0.0000	0.12850	0.99270	5.1888
0.050000	0.15230	1.1520	5.0616
0.10000	0.34480	2.1028	3.8425
0.15000	0.37320	4.7744	4.0284
0.20000	0.26830	6.9621	6.3570

Frequency = 4000 Hz

SPLi = 110 dB

Mo	Absorption Coefficient	R pc	χ pc
0.0000	0.051900	0.44660	5.6882
0.050000	0.010300	0.087500	5.7257
0.10000	0.26280	1.5568	4.1425
0.15000	0.31980	3.2717	4.7614
0.20000	0.24380	4.6012	6.6423

SPLi = 1120 dB

Mo	Absorption Coefficient	R pc	χ pc
0.0000	0.052000	0.44070	5.6400
0.050000	0.028600	0.22730	5.4983
0.10000	0.25710	1.7137	4.3932
0.15000	0.31930	3.0255	4.7655
0.20000	0.24390	4.5420	6.6170

SPLi = 130 dB

Mo	Absorption Coefficient	R pc	χ pc
0.0000	0.053500	0.45670	5.6597
0.050000	0.047900	0.39540	5.5975
0.10000	0.22810	1.5265	4.5156
0.15000	0.31170	3.2160	4.5468
0.20000	0.24420	4.5843	6.6255

SPLi = 145 dB

Mo	Absorption Coefficient	R pc	χ pc
0.0000	0.086400	0.76880	5.6962
0.050000	0.086400	0.77930	5.7362
0.10000	0.13220	0.93950	4.9674
0.15000	0.31420	2.5874	4.4500
0.20000	0.25620	4.6384	6.3733

Frequency = 5000 Hz

SPLi = 110 dB

Mo	Absorption Coefficient	R/pc	X'p
0.0000	0.069500	0.48800	5.0860
0.050000	0.076900	0.60140	5.3605
0.10000	0.11380	0.68130	4.5953
0.15000	0.24420	1.7195	4.5565
0.20000	0.26630	2.6973	5.1809

SPLi = 120 dB

Mo	Absorption Coefficient	R/pc	X'p
0.0000	0.048800	0.33640	5.0766
0.050000			
0.10000	0.055000	0.35970	4.9310
0.15000	0.13040	0.92530	4.9694
0.20000	0.27100	2.6031	5.1436

Frequency = 6000 Hz

SPLi = 110 dB

Mo	Absorption Coefficient	R/pc	χ /pc
0.0000	0.10790	0.63530	4.5687
0.050000	0.12900	0.96510	5.1030
0.10000	0.093700	0.45890	4.1792
0.15000	0.25270	1.4440	4.1059
0.20000	0.31420	2.0548	4.1026

SPLi = 120 dB

Mo	Absorption Coefficient	R/pc	χ /pc
0.0000	0.10820	0.63720	4.5690
0.050000	0.12430	0.93930	5.1443
0.10000	0.13340	0.64770	4.0877
0.15000	0.25960	1.4800	4.0811
0.20000	0.31440	2.0797	4.1137

SPLi = 130 dB

Mo	Absorption Coefficient	R/pc	χ /pc
0.0000	0.10770	0.62560	4.5388
0.050000	0.13220	0.97270	5.0527
0.10000	0.14480	0.73510	4.1584
0.15000	0.25570	1.5387	4.1962
0.20000	0.31370	2.0530	4.1062

SPLi = 145 dB

Mo	Absorption Coefficient	R/pc	χ /pc
0.0000	0.097300	0.53900	4.4479
0.050000	0.11600	0.79540	4.9139
0.10000	0.11060	0.60060	4.3775
0.15000	0.19540	1.1771	4.3990
0.20000	0.29690	1.8335	4.0831